23rd IMEKO TC4 International Symposium
Electrical & Electronic Measurements Promote Industry 4.0
September 17-20, 2019，Xi'an, China

Uncertainty in uncalibrated microwave resonant measurements

K. Torokhtii[1], A. Alimenti[1], N. Pompeo[1] and E. Silva[1]

[1]*Department of Engineering, Roma Tre University, Rome, Italy, kostiantyn.torokhtii@uniroma3.it*

***Abstract* – We present an extended study on the uncertainty in resonant measurements. The uncertainty of the resonant frequency and quality factor was estimated. The effect of the use of uncalibrated resonant curve on uncertainty was extensively studied. For the uncalibrated data the systematic contribution to uncertainty was determined.**

Keywords* – Dielectric resonator, *Microwaves, Uncertainty

I. INTRODUCTION

Continuous interest in the microwave measurements brings to the realization of the industrial grade methods for the material characterization. A wide range of material properties could be characterized at microwaves. The main advantage of the microwave techniques is their high sensitivity. They are widely used for the measurements of the complex permittivity of the liquids [1] and solid dielectrics [2]. Since long time microwave techniques have been used for the surface impedance (Z_s) measurements of the conductors. In particular, the microwave dielectric resonator (DR) method is a standard for the measurements of Z_s of superconductors [3]. In connection with other techniques as d.c. measurements, it is able to show an even more complete picture of the microscopic properties [4]. In this article, we focus on the DR based measurement technique.

In the last years, Vector Network Analysers (VNA) became more accessible due to low-cost solutions [5, 6]. However, the quality of the measurements relies heavily on the calibration procedure. In the case of less-performant VNAs, the importance of calibration becomes even more relevant.

In some cases, calibration becomes an impossible operation. The notable case is when the device under test (DUT) is placed in a harsh or particularly difficult environment. An example is represented by measurements of materials or devices at low, cryogenic temperatures [7]. Apart from the complexity of the cryogenic measurement system, one of the main problems originates from the part of the microwave line inside the cryostat which could not be calibrated using the standard procedure. Here, the main role is played by the absence of microwave standards capable to keep their characteristics in the hostile environment. One of the solutions is to develop custom standards [8], but it often requires very advanced techniques and particular knowledge. Moreover, it becomes then rather difficult to associate the appropriate uncertainty with the measured quantity.

In this paper, we extend the analysis of the effect of the uncalibrated measurements [9] to the case of the complete response of a resonator given by both the resonant frequency (f_0) and the quality factor (Q). With respect to the previous study, where we focused on Q only (and then only on the losses), we here explore the effect of uncalibrated measurements of a resonant system on the uncertainty to be associated also to f_0. We use the same Hakki-Coleman (H-C) dielectric resonant system for the measurements as in [9].

II. VARIABLE-Q RESONATOR CELL

In this study, we aim to evaluate the measurement uncertainty when a microwave line, or a part of it, cannot be calibrated, as in the cryogenic scenario above depicted. We designed an "open" type H-C resonator operating at room temperature. We used phase stable microwave cables with female-female (F-F) connectors. We designed the DR cell to have the reference plane of the microwave cable connector near the border of the DR cell. Coupling was made by removable antennas inserted directly in the F connector. With this design, we were able to perform the calibration up to the reference plane of the F connectors. The DUT consists therefore in the resonator cell only, as desirable in an ideal setup. In this way, uncalibrated measurements can be compared with calibrated ones without any not-accounted for contributions and avoiding de-embedding issues [10].

In Fig. 1 the sketch of the measurement cell is shown. The dielectric resonator is cylindrical and loaded with a sapphire puck, chosen because of its low dielectric losses and high permittivity. The latter allows to concentrate the electromagnetic field within and near the dielectric puck. A mono-crystal sapphire puck with diameter 8 mm and height 4.5 mm was used. An Anritsu 37269D VNA with 60 cm phase stable Anritsu cables was used for measurements and connections.

We are interested in the evaluation of the uncertainty

in the measurements of the resonator parameters with different quality factors Q. We then designed a system for measurements in a wide range of Q-factors in the same conditions, which include, in particular, the frequency range of operation of the DR.

In order to change the Q values of the resonator in a controlled way, we both substituted the bases using metals with different resistivities and changed the position of the upper base and thus the height of the corresponding gap of the DR. By fine tuning the latter, we were able to keep the resonant frequency within a chosen fixed range.

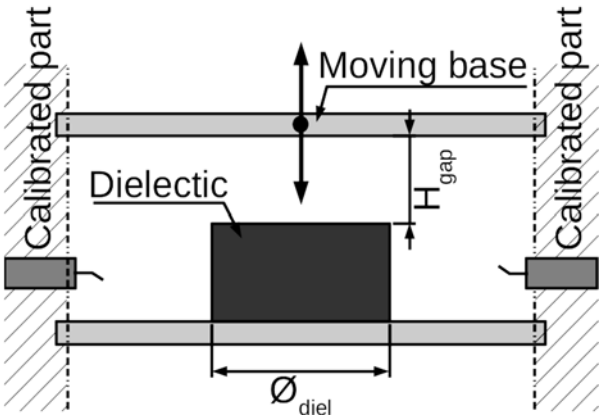

Fig. 1 Variable-Q resonant cell.

III. Q-FACTOR AND RESONANT FREQUENCY EXTRACTION

Q and f_0 are important properties of a resonator. As an example, when a resonator is used to determine the surface impedance of a material, the quality of measurements of the surface impedance Z_s=R_s+i X_s by the resonant method depends directly on f_0 and Q. Usually, the variation of the surface impedance with some external parameter is obtained experimentally, while the determination of the absolute value of Z_s is a more complex issue due to the absence of the reference material with known X_s. The relation between Z_s and resonant parameters is the following [11]:

$$\Delta Z_S = \Delta R_S + i\Delta X_S = G\Delta\frac{1}{Q} - 2iG\frac{\Delta f_0}{f_0} + bg \quad (1)$$

where G is the constant called geometrical factor, and the background "bg" is the contribution of the resonator without the sample. From Eq.(1) it is clear how the uncertainty of Z_s originates mainly from $u(Q)$, Q, $u(f_0)$ and f_0 ($u(G)$, as obtained by simulation, is usually <1%), whence the interest in the estimate of $u(Q)$ and $u(f_0)$.

In a resonator working in transmission f_0 and Q can be obtained based on the measurements of the complex-valued transmission coefficient (S_{21}). While preliminary estimates for Q and f_0 can be obtained by the so-called -3dB method, a more precise approach is to use an appropriate fit of the resonance curve. In [12] it was shown that a Lorentzian curve can be used to fit the function $|S_{21}|(f)$ only for "ideal" case. The real resonator includes corrections connected to cross-coupling and phase contributions. The resonance curve can be described through the following general equation ("Fano resonance model" [13]) with a phase correction:

$$S_{21}(f) = \left[\frac{S_{21}(f_0)}{1-2iQ\frac{f-f_0}{f_0}} + S_c\right]e^{i\varphi} \quad (2)$$

where $S_{21}(f_0)$ is the transmission S-parameter at the resonant frequency, S_c represents the contribution originated from the cross-coupling and $e^{i\varphi}$ is the phase correction.

There is a huge number of methods for the extraction of f_0 and Q from the experimental data [14]. A widely used method is the so-called circular fit approach [15], but it is also possible to use a complex-valued modification of Levenberg-Marquardt algorithm to fit the complex S_{21} [16]. However, complex-valued fitting requires more calculation power and custom algorithms. Additional complexities arise when the uncertainty of the fitting parameters must be estimated. From this point of view the fit of the modulus of S_{21} remains more accessible due to already implemented algorithms in popular programming languages such as Python and MATLAB [17]. Using the fit of $|S_{21}(f)|$ one can implement a fitting procedure with cheap computers like the Raspberry Pi. $|S_{21}(f)|$ is obtained from Eq.(2) as:

$$|S_{21}|^2(f) = \frac{S_{21}(f_0)}{1+4Q^2\left(\frac{f-f_0}{f_0}\right)^2}\Big[S_{21}(f_0) + 2\Re(S_c) + 4Q\frac{f-f_0}{f_0}\Im(S_c)\Big] + \Re^2(S_c) + \Im^2(S_c) \quad (3)$$

The fitting algorithm include then 5 independent parameters.

IV. MEASUREMENT PROCEDURE

In this section, we present an extended elaboration of the measurement procedure presented in [9]. The aim was to complete the estimate of the uncertainty of the measurements of the characteristic parameters of a resonator for uncalibrated measurements, including also the resonant frequency.

We performed experimental measurements in a wide range of Q factor, with very small variations of other controlled parameters of the resonant system. The interest is the comparison between the Q and f_0 measurements obtained with and without the VNA calibration.

First, we fixed the calibration in the narrow frequency band 13.17-13.26 GHz, chosen to accommodate all the Q–varying resonant curves to be measured with sufficient frequency points density, with 1601 calibrated points (the maximum number of data-points for the Anritsu 37269D

VNA). The calibration was performed by the standard 12-term SOLT (Short-Open-Load-Thru) calibration procedure by the algorithms incorporated in VNA. Here, for the experimental measurements, we followed Anritsu 37269D VNA calibration guide.

Then, resonance curves were recorded with Q-factor varied in the range 2000 – 9500. To obtain such a wide range of Q with the same setup we change the air gap and we use different metals for the bases, as explained before. The gap, controlled by only one movable part of the resonator cell– the upper base (See Fig. 1), allowed to tune the operating resonance frequency to be always within the "calibrated" frequency range.

For each fixed position of the upper base, two measurements were performed: with and without calibration applied. In Fig. 2 an example of the measured calibrated and uncalibrated resonant curve is shown. The difference is immediately appreciated, confirming the need to assess the quality of an uncalibrated measurement even for a resonant device (naïvely, one could expect that resonant systems are sufficiently narrowband to be nearly insensitive to the calibration).

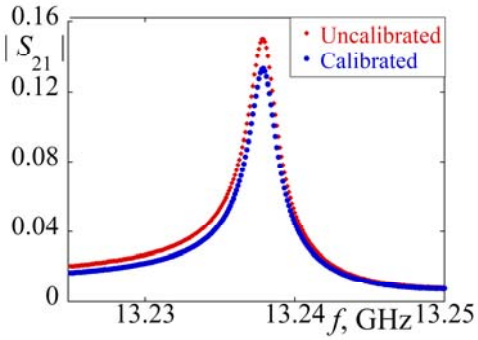

Fig. 2. Measured resonant curves with and without calibration applied.

V. RESULTS

A series of resonant curves was recorded, and fits by Eq.(2) were applied to raw data and to calibrated data. Care was taken in order to have similar fit conditions. It should be noted that in our situation the step between measured points was constant for all measurements. Since Q changes significantly, without proper "normalizations" the fits of the curves with low and with high Q would have not been in the same conditions for what concerns the density of information per interval.

Therefore, we proceeded as follows. First, we limited the span of each curve to $N\Delta f_{FWHM}$, where Δf_{FWHM} is the full-width half maximum frequency range, and N>1 is a proper multiplicative factor. In our case, N was constrained by the available frequency range of the calibration and hence set equal to 5. The resulting curves, having different frequency spans with frequency points evenly spaced, had at this step different numbers of points. Each set was then trimmed uniformly, in order to have as much as possible the same amount of evenly spaced data-points. As a result, in the range of Q=2000-9500 we obtained the final set of the resonant curves, trimmed and with same information density, with span $5\Delta f_{FWHM}$ and data-points in the range 222-286. We now discuss the elaboration of this set of curves.

Resonant curves were fitted using Eq.(3). It should be noted that the uncertainty $u(|S_{21}|)$ could be estimated only for the calibrated curve [9], according e.g. to the estimates given by the "Exact Uncertainty Calculator" proprietary software tool by Anritsu [18] (although alternative tools like in [19] could be used). This tool estimates automatically uncertainties for all S-parameters taking into account the characteristics of the VNA, cables, connectors and calibration kit. The worst case of uncertainty on S_{21}, in the conditions of this study, is <1% for calibrated measurements. For uncalibrated curves zero uncertainty in $|S_{21}|$ had to be used.

A widely used Levenberg-Marquardt [16] fit algorithm implementation in Python provides a variance vector of the fit parameters through the numerically calculated Jacobian (more details can be found in ref. [17, 20]). Q and f_0 uncertainties were estimated as the square root of the corresponding fitting parameters variances. Moreover, as a consequence of the non-application of the calibration, systematic effects as significant sources of uncertainty are expected. Thus, we define as a measure of this uncertainty the discrepancy between the resonant parameters as derived by the fitting of calibrated and uncalibrated curves. The discrepancy of Q could be defined as the relative variation between Q obtained from calibrated (Q_{cal}) and uncalibrated (Q_{uncal}) data, $(Q_{uncal} - Q_{cal})/Q_{cal}$. For f_0 the discrepancy is defined in the same manner as $(f_{0,uncal} - f_{0,cal})/f_{0,cal}$ where $f_{0,uncal}$ and $f_{0,cal}$ are the resonant frequencies obtained by the fit of uncalibrated and calibrated curves, respectively.

In Fig. 3 and Fig. 4 the relative uncertainties of Q-factors and resonant frequencies f_0 are shown.

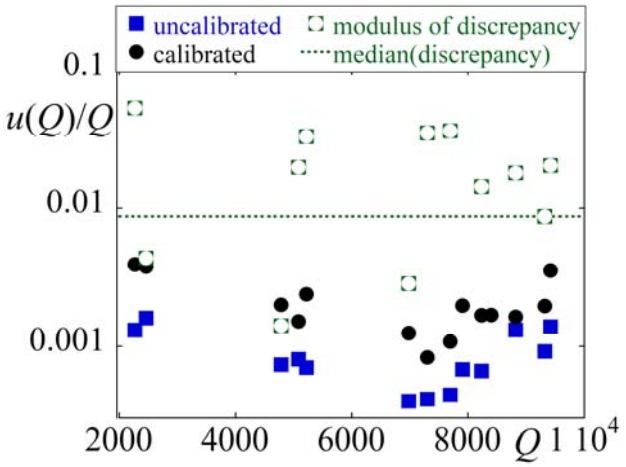

Fig. 3. Relative uncertainty on calibrated Q–factor compared to the systematic error $(Q_{uncal} - Q_{cal})/Q_{cal}$.

The uncertainties of the uncalibrated measurements, with $u(|S_{21}|) = 0$, include only the contribution of the uncertainty of the fit algorithm.

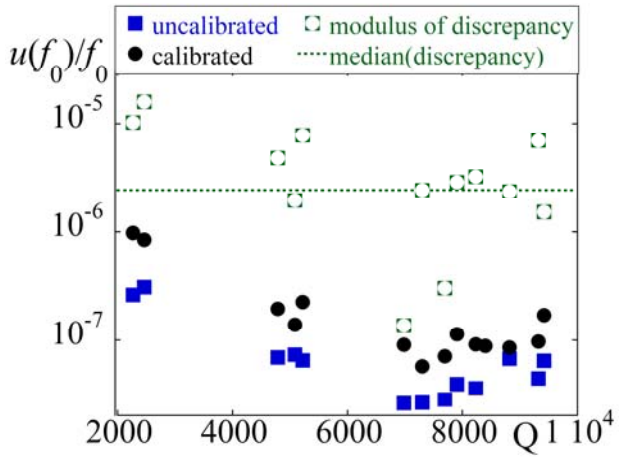

Fig. 4. Relative uncertainty on calibrated resonant frequency compared to the systematic error ($f_{0,uncal}$ - $f_{0,cal}$)/ $f_{0,cal}$.

For Q-factor the relative uncertainty $u(Q)/Q$ is below 0.17 %, for f_0 the uncertainty $u(f_0)/f_0$ is below 0.32 ppm. Considering the calibrated values of $u(|S_{21}|)$, the uncertainty of Q and f_0 become $u(Q)/Q < 0.4$ % and $u(f_0)/f_0 < 1$ ppm.

As far as the systematic effects are concerned, the comparison of the fit parameters between calibrated and uncalibrated cases yields median values equal to 0.87 % for the discrepancy in Q and equal to 2.5 ppm for the discrepancy in f_0. It has to be noted that discrepancies can be both positive and negative. In Figures 3 and 4 both the discrepancies (in modulus) and their median are shown. Considering the worst-case values as the estimate of the maximum systematic contribution to uncertainty, we obtain values equal to 5.4 % for Q and 16 ppm for f_0.

VI. CONCLUSIONS

We performed an extended study on the measurement uncertainty on the Q-factor and resonant frequency f_0 of microwave resonator, arising when the microwave line is not calibrated. By exploring a wide range of Q-factors, made possible by the implementation of an ad-hoc resonator cell, we compared the results obtained with calibrated and uncalibrated data. After proper "normalizations" of the data sets, in terms of frequency spans and points number, we discover that while for the calibrated curves the uncertainty is below 0.4 % for Q and below 1 ppm for f_0, in the uncalibrated measurements a systematic contribution is dominant. By estimating this contribution from the discrepancy between the fit results of calibrated and uncalibrated data, we obtain an experimental quantification of the systematic contribution equal to 5.4 % for Q and 16 ppm for f_0. These results provide a guide for the evaluation of the uncertainty contribution to be taken into account when calibration of microwave lines similar to the one studied are not feasible.

REFERENCES

[1] Chen, S. et al., *A Dielectric Constant Measurement System for Liquid Based on SIW Resonator*, IEEE Access, vol. 6, July 2018, pp. 41163 - 41172.

[2] Schultz, J. W., *A New Dielectric Analyzer for Rapid Measurement of Microwave Substrates up to 6 GHz*, Proc. of AMTA 2018, Williamsburg, 4-9 Nov, 2018, pp. 1-6.

[3] IEC 61788-7:2006, *Superconductivity - Part 7: Electronic characteristic measurements - Surface resistance of superconductors at microwave frequencies*.

[4] Frolova, A. et al., Critical current and vortex pinning properties in $YBa_2Cu_3O_{7-x}$ films with Ba_2YTaO_6+Ba_2YNbO_6 and $BaZrO_3$ nanoinclusions by DC transport and microwave measurements, IEEE Trans. Appl. Supercond., vol. 28, no. 4, June 2018, Art. ID 7500805

[5] Will, K., Meyer, T. and Omar, A., *Low-cost high-resolution handheld VNA using RF interferometry*, 2008 *IEEE MTT-S International Microwave Symposium Digest*, 15-20 June, 2008, pp. 375-378.

[6] Sokoll, T. and Jacob, A. F., *Self‐calibration circuits and routines for low‐cost measuring systems*, *Microw. Opt. Technol. Lett., vol.* 50, no. 2, February 2008, pp. 287-293.

[7] Alimenti, A. et al., *Surface Impedance Measurements on Nb3Sn in High Magnetic Fields*, IEEE Trans. Appl. Supercond., vol. 29, no. 5, January 2019, Art. ID 3500104.

[8] Scheffler, M. and Dressel, M., *Broadband microwave spectroscopy in Corbino geometry for temperatures down to 1.7 K*, *Rev. Sci. Instrum. vol.* 76, *June 2005,* Art. ID 074702; Scheffler, M. et al., *Broadband Corbino spectroscopy and stripline resonators to study the microwave properties of superconductors*, Acta IMEKO, vol 4, no 3, 2015, pp. 47-52.

[9] Torokhtii, K. et al., *Q-factor of microwave resonators: calibrated vs. uncalibrated measurements*, J. Phys. Conf. Ser., vol. 1065, no. 5, June 2005, Art. ID 052027.

[10] *Embedding/De-embedding*, Anritsu Application Note, May 2002

[11] Pompeo, N., Torokhtii, K., Silva, E., *Dielectric resonators for the measurements of the surface impedance of superconducting films*, Meas. Sci. Rev., vol, 14, no. 3, June 2014, pp. 164-170.

[12] Pompeo, N. et al., *Fitting strategy of resonance curves from microwave resonators with non-idealities*, Proc. of I2MTC 2017 - 2017 IEEE International Instrumentation and Measurement Technology Conference, J. Phys. Conf. Ser., Torino; 22 - 25 May 2017, pp. 1-6

[13] Yoon, J. W. and Magnusson, R., *Fano resonance formula for lossy two-port systems*, Opt. Express, vol. 21, no 15, 2013, pp. 17751-17759.

[14] Petersan, P. J. and Anlage, S. M., *Measurement of resonant frequency and quality factor of microwave resonators: Comparison of methods*, J. Appl. Phys., vol 84, no. 6, September 1998, pp. 3392–3402.

[15] Leong, K. and Mazierska, J., *Precise measurements of the Q factor of dielectric resonators in the transmission mode-accounting for noise, crosstalk, delay of uncalibrated lines, coupling loss, and coupling reactance*, Meas. Sci. Rev., vol. 50, no. 9, September 2002, pp. 2115–2127.

[16] Žic, M., *An alternative approach to solve complex nonlinear least-squares problems*, J. Electroanal. Chem., vol. 760, January 2016, pp. 85 – 96.

[17] More, J. J., Garbow B. S. and Hillstrom K. E.., *User Guide for MINPACK-1*, Argonne National Laboratory, Argonne, Ill., 1980.

[18] www.anritsu.com

[19] Wollensack, M., Hoffmann, J., Ruefenacht, J. and Zeier, M., *VNA Tools II: S-parameter uncertainty calculation*, Proc. in 79th ARFTG Microwave Measurement Conference, Montreal, 22 June 2012, pp. 1-5.

[20] Jones E, Oliphant E, Peterson P, et al., SciPy: Open Source Scientific Tools for Python, 2001, https://docs.scipy.org/doc/scipy/reference/generated/scipy.optimize.curve_fit.html

.